

# A Wave-Envelope Technique for Wave Propagation in Nonuniform Ducts

J. E. Kaiser\* and A. H. Nayfeh†

Virginia Polytechnic Institute and State University, Blacksburg, Va.

The method of variation of parameters is used to analyze wave propagation in variable area, plane ducts with no mean flow. The method has an explicit representation of the fast axial variation of the acoustic modes, and numerical integration is required only for the slower axial variations of the mode amplitudes and phases. Results are presented which demonstrate the numerical advantages of the method. Comparison of the results with those of a small perturbation theory are given. The relationship between this method and the method of weighted-residuals is discussed.

## I. Introduction

A NUMBER of methods have been developed for calculation of acoustic propagation in ducts of variable cross section.<sup>1</sup> These methods include direct numerical analysis,<sup>2</sup> multiple-scale solutions for slowly-varying cross sections,<sup>3-5</sup> and weighted-residual analyses,<sup>6,7</sup> among others. Each approach has unique characteristics and advantages, as well as obvious limitations, either of a numerical or physical nature. For example, no tests have been made to establish the range of geometry variations for which the multiple-scale solutions remain valid; direct numerical analyses require small step sizes and large computation times for high frequencies and high-order modes because of the rapid axial and transverse oscillations; and weighted-residual analysis<sup>7</sup> also requires a numerical integration over each axial oscillation of the signal although the transverse variations of high-order modes present no difficulty.

The computation of these axial variations has been simplified in a direct numerical analysis of wave propagation in constant-area ducts by using an estimate of the harmonic axial variations of the fundamental mode.<sup>8</sup> This procedure was reportedly advantageous even with estimates that were only moderately accurate.

In the work reported here, acoustic propagation in variable-area ducts without mean flow is analyzed by the method of variation of parameters<sup>9</sup> in a manner that incorporates features of several previous investigations. To facilitate the study of high-order modes and multimodal interactions, the acoustic disturbance is represented as a superposition of parallel-duct eigenfunctions. Moreover, the fast axial variation is given explicitly, and numerical integration is required only for the slower axial variations of the amplitudes and the phases of the modes. We have borrowed the term 'wave-envelope method' as a description of this aspect of the method, although in most respects it bears little resemblance to the procedure used by Baumeister.<sup>8</sup> Finally, the representation of the acoustic wave is required to satisfy an integrability constraint derived from the wave equation; this feature is similar to that used in the multiple-scale analysis by Nayfeh and Telionis,<sup>3</sup> but does not have the small perturbation limitation.

The numerical results from the wave-envelope analysis are compared with those obtained from a standard weighted-residual approach to determine the extent of the numerical

advantage. A comparison with the multiple-scale results for a range of geometry variations provides some guides on the range of validity of that method. In addition, the relation between the integrability constraint and the weighted-residual constraint is discussed.

## II. Problem Formulation

Sound propagation in a plane duct with no mean flow is considered. The upper wall is lined, and the lower wall is rigid; see Fig. 1. The basis of the analysis is the reduced wave equation

$$\frac{\partial^2 p}{\partial y^2} + \frac{\partial^2 p}{\partial x^2} + \omega^2 p = 0 \quad (1)$$

together with the boundary conditions

$$\frac{\partial p}{\partial y} \cos \theta - \frac{\partial p}{\partial x} \sin \theta - i\omega\beta p = 0 \text{ at } y = b(x) \quad (2)$$

$$\frac{\partial p}{\partial y} = 0 \quad \text{at } y = 0 \quad (3)$$

where the acoustic disturbance is  $p \exp(-i\omega t)$ ,  $\beta$  is the liner admittance,  $b$  is the duct width, and  $\tan \theta$  is the slope of the upper wall. All variables are nondimensional; the duct width at  $x=0$ , the mean density, and the mean speed of sound provide the basic reference quantities.

The solution to Eqs. (1-3) is approximated by a finite sum of the parallel-duct eigenfunctions

$$p \sim p_N = \sum_{n=1}^N \left( F_n(x) \exp(i \int k_n dx) + G_n(x) \exp(-i \int k_n dx) \right) \cos \kappa_n y \quad (4)$$

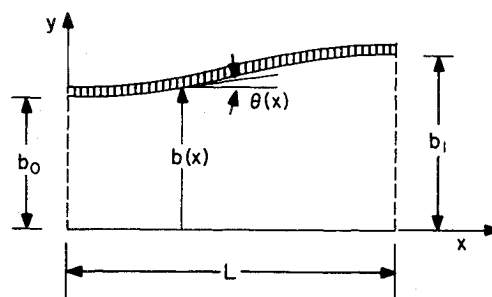


Fig. 1 Duct geometry.

Presented as Paper 76-495 at the Third AIAA Aero-Acoustics Conference, Palo Alto, Calif., July 20-23, 1976; submitted Sept 13, 1976; revision received Dec. 20, 1976.

Index category: Aircraft Noise, Powerplant.

\*Associate Professor, Department of Engineering Science and Mechanics. Member AIAA.

†University Distinguished Professor, Department of Engineering Science and Mechanics. Member AIAA.

where  $\kappa_n$ ,  $n = 1, 2, \dots, N$ , are the roots of

$$\kappa_n \sin \kappa_n b = -i\omega\beta \cos \kappa_n b \quad (5)$$

and

$$k_n = (\omega^2 - \kappa_n^2)^{1/2} \quad (6)$$

are the complex propagation constants. The moduli and arguments of  $F_n$  and  $G_n$  are, respectively, the amplitudes and the phases of the right-running and left-running modes. Since  $k_n$  is complex the exponential factors contain an estimate of the attenuation rates of the modes; thus, the values of  $F_n$  and  $G_n$  do not form the actual wave envelopes but simply provide a measure of the variation of the mode parameters from the quasiparallel values. This variation-of-parameters method has also been called the 'special perturbation method' in studies of astronomy problems (see Ref. 9 for literature citations).

Since the transverse dependence in Eq. (4) is chosen a priori,  $p_N$  cannot satisfy Eqs. (1) and (2) exactly. Thus, the function  $p_N$  is subjected to an integrability constraint that is derived from Eqs. (1-3). Equation (1) is multiplied by a function  $\phi$  and integrated across the duct width. The  $y$ -derivatives are integrated by parts, and Eqs. (2) and (3) are used to simplify the resulting boundary terms. Finally  $\phi$  is defined to be the solution to the adjoint problem

$$\frac{\partial^2 \phi}{\partial y^2} + \kappa_n^2 \phi = 0$$

$$\frac{\partial \phi}{\partial y} = i\omega\beta \phi \text{ at } y = b(x)$$

and

$$\frac{\partial \phi}{\partial y} = 0 \text{ at } y = 0$$

Thus the function  $\phi$  is given by the quasiparallel eigenfunctions,  $\cos \kappa_n y$ . With the above manipulations, one finds that any solution to Eqs. (1-3) must also satisfy the constraints

$$\int_0^b \frac{\partial^2 p}{\partial x^2} \cos \kappa_n y dy + k_n^2 \int_0^b p \cos \kappa_n y dy$$

$$= [(\cos \theta - 1) i\omega\beta p / \cos \theta - \frac{\partial p}{\partial x} \tan \theta]_{y=b} \cos \kappa_n b \quad (7)$$

for all values of  $\kappa_n$ . The approximate solution  $p = p_N$  is required to satisfy these integrability conditions.

The method of weighted residuals, as used in Ref. 7, involves steps similar to those described above, except that the basic conservation laws are used instead of the wave equation. It is instructive to examine the relation between the method of weighted residuals (MWR) and the integrability approach for the problem posed by Eqs. (1-3). Substitution of Eq. (4) into Eqs. (1) and (2) leads to errors or "residuals"; thus,

$$\sigma_1(x, y) = \frac{\partial^2 p_N}{\partial y^2} + \frac{\partial^2 p_N}{\partial x^2} + \omega^2 p_N \quad (8)$$

and

$$\sigma_2(x) = \left[ -\frac{\partial p_N}{\partial y} \cos \theta + \frac{\partial p_N}{\partial x} \sin \theta + i\omega\beta p_N \right]_{y=b} \quad (9)$$

are the residuals of the wave equation and the liner boundary condition, respectively. Following the usual approach for weighted residuals,<sup>10</sup> one requires that  $\sigma_1$  be orthogonal to the set of functions  $\cos \kappa_n y$  as a "minimization" principle. In-

tegrating the  $y$ -derivatives by parts and substituting for boundary terms from Eq. (9), one finds that

$$\int_0^b \sigma_1 \cos \kappa_n y dy + \sigma_2 \cos \kappa_n b / \cos \theta = 0 \quad (10)$$

leads to Eq. (7) as the weighted residual equation. Thus, for this problem, a requirement that the weighted average of the residuals vanish is the same as requiring that the approximation satisfy the integrability constraints for the actual solution.

However, this close parallel between the two formulations does not exist when one attempts to solve a system of equations (for example, in the case when there is a mean flow). In such a case, the adjoint of the system of equations must be defined, and the single integrability constraint developed from the system of equations. The resulting problem statement is simpler than that which is obtained from the standard weighted-residual approach, involving fewer unknowns and equations. This approach is now under investigation for propagation in circular ducts carrying a high-speed mean flow; the results of this study will be reported at a future date.

### III. Solution

Since two parameters,  $F_n$  and  $G_n$ , are introduced for each mode eigenfunction, one is free to choose one additional constraint in addition to Eq. (7). In this problem we require that the axial velocity also be represented by a superposition of the right- and left-running quasiparallel duct modes by setting

$$\frac{\partial p}{\partial x} = \sum_{n=1}^N i k_n [F_n(x) E_n - G_n(x) / E_n] \cos \kappa_n y$$

which leads to the conditions

$$\frac{dG_n}{dx} = -\frac{dF_n}{dx} E_n^2, \quad n = 1, 2, \dots, N \quad (11)$$

where

$$E_n \equiv \exp(i \int k_n dx) \quad (12)$$

Substituting Eq. (4) into Eq. (7) and using Eq. (11), one obtains an equation of the form

$$\frac{dF_n}{dx} + \frac{1}{N_n} \frac{d}{dx} (L n \sqrt{k_n N_n}) (F_n E_n - G_n / E_n)$$

$$= \sum_{m=1}^N \tilde{U}_{mn} F_m + \sum_{m=1}^N \tilde{V}_{mn} G_m \quad (13)$$

where

$$N_n = \int_0^b \cos^2 \kappa_n y dy = \frac{1}{2} \left[ b + \frac{\sin 2\kappa_n b}{2\kappa_n} \right] \quad (14)$$

and the mode-coupling coefficients  $\tilde{U}_{mn}$  and  $\tilde{V}_{mn}$  are given in the Appendix. Equations (11) and (13) are the ordinary-differential equations that are solved for the axial variation of the mode parameters  $F_n$  and  $G_n$ . For comparison, a standard weighted residual solution to Eq. (7) is also obtained in the form

$$p = \sum_{n=1}^N p_n(x) \cos \kappa_n y \quad (15)$$

Substituting Eq. (14) into Eq. (7), one obtains

$$\frac{d^2 p_n}{dx^2} + \frac{1}{N_n} \frac{dN_n}{dx} \frac{dp_n}{dx} + k_n^2 p_n$$

$$= \sum_{m=1}^N U_{mn} p_m + \sum_{m=1}^N V_{mn} \frac{dp_m}{dx} \quad (16)$$

where the coupling coefficients  $U_{mn}$  and  $V_{mn}$  are given in the Appendix.

From the equations in the Appendix, one can note that the mode coupling coefficients are proportional to the axial derivatives of  $\kappa_n$ , which, in turn, are related to the axial derivatives of the duct width and the liner admittance. Thus, integration of Eqs. (11) and (13) or Eq. (16) will yield mode-coupling effects that are proportional to the overall changes in the duct properties. For ducts with moderate axial variations, Eq. (16) describes a harmonic oscillator with weak forcing terms from the other modes. Consequently, for high frequencies, the numerical solution of Eq. (16) will require small step sizes to describe the harmonic variation of  $p_n$  over each wave length. On the other hand, Eqs. (11) and (13) describe variables that differ from a constant only as a consequence of the axial variations of the duct properties. Thus, the wave-envelope description should be considerably more efficient than the description in Eq. (15), except at low frequencies.

Following Ref. 11, results are obtained in the form of transmission and reflection coefficients for the variable-area segment being considered. To this end, Eqs. (11–13), or (16), are solved numerically using a standard Runge-Kutta procedure to determine the transfer matrices  $TR_1$ ,  $TR_2$ ,  $TR_3$ , and  $TR_4$  that relate the mode amplitudes at  $x=0$  to those of  $x=L$

$$A^+(L) = TR_1 A^+(0) + TR_2 A^-(0)$$

$$A^-(L) = TR_3 A^+(0) + TR_4 A^-(0) \quad (17)$$

where  $A^+(x)$  is a column vector of the amplitudes  $F_n E_n$  of the right-running modes and  $A^-(x)$  is a column vector of the amplitudes  $G_n/E_n$  of the left-running modes. The transmission and reflection coefficients relate the magnitudes of the outgoing modes to those of the incoming modes

$$A^+(L) = T^{L,0} A^+(0) + R^{L,L} A^-(L)$$

$$A^-(0) = T^{0,L} A^-(L) + R^{0,0} A^+(0) \quad (18)$$

and are calculated from the transfer matrices by

$$T^{0,L} = TR_4^{-1}$$

$$R^{0,0} = -TR_4^{-1} TR_3$$

$$R^{L,L} = TR_2 TR_4^{-1}$$

$$T^{L,0} = TR_1 + TR_2 R^{0,0} \quad (19)$$

(The reflection coefficients are the negative of those defined in Ref. 11 as a consequence of the use of the positive sign on the  $G_n$  term in Eq. (4)). The  $(m,n)$  term of  $T^{L,0}$  represents the

transmission of the  $m$ (th) mode at  $x=L$  due to the  $n$ (th) mode incident at  $x=0$ , etc.

For purposes of comparison with the results of previous investigations, the computer programs were constructed to permit the calculation of the effects of discontinuous liner properties at the duct entrance and exit as described in Ref. 11 and to combine these effects with the variable-area effects to obtain overall transmission and reflection coefficients. However, the primary concern of this investigation was to examine the influence of the variable area.

#### IV. Numerical Results

The duct configuration used for the numerical study is depicted in Fig. 1. The upper wall follows a cosine variation from a width  $b_0$  at  $x=0$  to  $b_1$  at  $x=L$ . The liner admittance can vary from  $\beta_0$  at  $x=0$  to  $\beta_1$  at  $x=L$  according to a cubic variation that gives  $d\beta/dx=0$  at the entrance and at the exit.

When the effects of the liner discontinuities are included, the wave-envelope results agree to three significant figures with those of Ref. 7. The numerical convergence of the results with an increasing number of modes is documented in Ref. 7 and is not repeated here.

Considering only the effect of the area variation, we have compared the rate of numerical convergence with step size of the wave-envelope method with the standard weighted residual method. Table 1 provides a comparison of  $T_{11}^{0,L}$  for a case in which the maximum wall slope is approximately 0.24; other coefficients show similar behavior. At low frequencies the two methods are nearly equivalent and few steps are required for three-place accuracy. However, as the frequency increases the standard weighted residual method converges more slowly, whereas the wave-envelope results are nearly independent of the step size. Figure 2 shows a comparison of

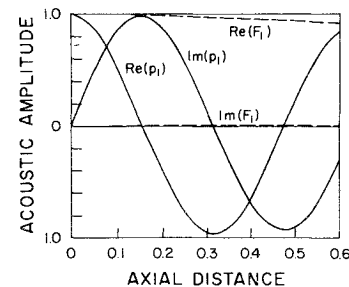


Fig. 2 Comparison of two methods for calculation of acoustic amplitudes; first mode incident from the left;  $\omega=10$ ,  $b_0=1.0$ ,  $b_1=1.20$ ,  $L=1.0$ ,  $\beta=0.6-0.4i$ ,  $N=4$ .

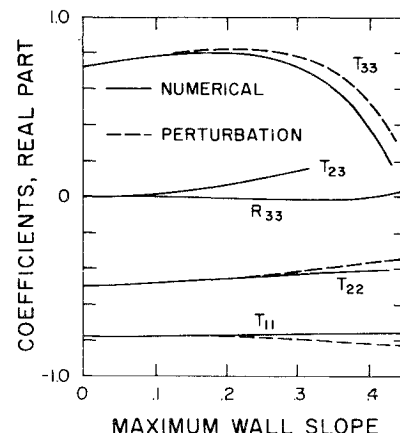


Fig. 3 Comparison of the real parts of the transmission and reflection coefficients with the results from a small-perturbation theory;  $\omega=9$ ,  $b_0=1.0$ ,  $L=1.0$ ,  $\beta=0.2-0.1i$ ,  $N=6$ .

Table 1 Comparison of convergence of wave-envelope and weighted residuals methods<sup>a</sup>

$\omega$	$\Delta x$	$T_{11}^{0,L}$	
		Wave-envelope	MWR
3	.2	-.5003 + .1463i	-.5010 + .1479i
	.1	-.5003 + .1456i	-.5001 + .1461i
	.05	-.5003 + .1452i	-.5001 + .1454i
	.02	-.5003 + .1449i	-.5002 + .1451i
10	.2	-.9391 - .4539i	-3.59 - 2.21i
	.1	-.9397 - .4540i	-1.019 - .4267i
	.05	-.9398 - .4539i	-.9438 - .4511i
	.02	-.9398 - .4539i	-.9400 - .4541i
20	.2	.4896 + .9398i	0
	.1	.4861 + .9406i	3.784 + 19.30i
	.05	.4892 + .9407i	.6651 + .9922i
	.02	.4892 + .9407i	.4932 + .9404i

<sup>a</sup>  $b_0=1.0$ ,  $b_1=1.15$ ,  $L=1.0$ ,  $\beta=0.6-0.4i$ ,  $N=4$ .

the calculation of the first right-running mode by the two methods for a maximum wall slope of 0.31. The advantage of the wave-envelope method is apparent. The variation of  $F_n$  is stronger in some situations, but in all cases considered for this study (maximum wall slopes up to approximately 0.5) the wave-envelope method was considerably better except at low frequencies where it was just as good.

In Fig. 3, several transmission coefficients are compared with those predicted by the multiple-scale analysis of Ref. 3. To the leading approximation, the multiple-scale results predict that the direct transmission coefficients are

$$T_{nn}^{L,0} = [k_n(0)N_n(0)/k_n(L)N_n(L)]^{1/2} \exp[i \int_0^L k_n dx]$$

$$T_{nn}^{0,L} = [k_n(L)N_n(L)/k_n(0)N_n(0)]^{1/2} \exp[i \int_0^L k_n dx]$$

and the intermodal coupling is a higher-order effect. For simplicity, only the real part of the coefficients is shown, and only coefficients for modes incident from the left are shown. The direct transmission coefficients predicted by the first-order perturbation theory remain within a few percent of the numerical results for maximum wall slopes up to a value of 0.2, and even at larger values the proper trend is shown as the third mode approaches cutoff. The reflection coefficients do not differ greatly from the zero value predicted by the perturbation analysis. However, the biggest disadvantage of the first-order perturbation theory is the inability to calculate the intermodal coupling in transmission. This coupling appears to be somewhat stronger for waves moving into a converging channel than for a diverging channel and first appears at fairly small values of the wall slope. An extension of the perturbation theory to higher order could be helpful in identifying the mechanisms that are operating.

The small values of the reflection coefficients cited above are generally consistent with the other cases that have been examined (it is re-emphasized that we are considering only the effect of the variable area). For example, Table 2 shows reflection coefficients,  $R_{s,n}^{0,L}$ , in mode 5 due to several right-running modes incident from the left on an expanding section. The fifth mode is right at the cut-on frequency at the duct entrance. Clearly, the large reflection coefficients that were reported in Ref. 7 for this case are a result of matching at the liner discontinuity, and the mode coupling within the variable-area section is relatively minor. Also shown are the transmission and reflection characteristics for the sixth mode entering the converging channel from the right. Mode 6 is cut on at  $x=L$  and is cut off at  $x=0$ . The direct reflection coefficient is the dominant coefficient and the intermodal coupling is very weak.

For small wall slopes, such as those that would be encountered in a duct that carries a high-speed mean flow, it appears possible that much of the intermodal coupling in reflection and some of the coupling in transmission could be neglected without introducing appreciable errors. This is important for computational efficiency since the time requirements increase rapidly with an increasing number of

Table 2 Reflection and transmission characteristics of two modes near cutoff conditions<sup>a</sup>

$n$	$R_{s,n}^{0,0}$	$R_{n,6}^{L,L}$	$T_{n,6}^{0,L}$
1	.000 - .000i	.001 + .000i	.000 + .001i
2	-.001 + .000i	.004 - .001i	-.004 - .005i
3	.001 - .001i	-.013 + .010i	.028 - .001i
4	-.002 + .001i	.019 - .065i	.023 - .060i
5	.028 + .009i	.002 + .001i	.001 + .001i
6	-.001 + .001i	.188 + .033i	.003 + .003i

<sup>a</sup> $\omega = 12.57$ ,  $b_0 = 1.0$ ,  $b_1 = 1.268$ ,  $L = 1$ ,  $\lambda_0 = \beta_1 = .776 - .31i$ ,  $N = 10$ , max. wall slope = 0.42.

Table 3 Influence of transition length on magnitudes of transmission coefficients<sup>a</sup>

$L$	$ T_{11} $	$ T_{12} $	$ T_{13} $
0	1.28	.324	.069
0.1	1.26	.319	.068
0.2	1.25	.318	.068
0.4	1.24	.314	.067
0.6	1.22	.311	.065
0.8	1.21	.307	.062
1.0	1.19	.304	.059

<sup>a</sup> $\omega = 9$ ,  $\beta_1 = 0$ ,  $\beta_2 = 0.2 - 0.1i$ ,  $b_1 = b_2 = 1.0$ ,  $N = 6$ .

modes. The modes that produce the largest reflection coefficients are those for which  $N_n$  becomes large. A mode whose eigenvalue  $\kappa_n$  has a large imaginary part has a value of  $N_n$  proportional to  $\exp[2\text{Im}(\kappa_n)]$ , and such a mode usually has large reflection coefficients into other modes. However, this is simply a consequence of working with the eigenfunctions  $\cos \kappa_n y$  rather than normalized functions for which  $N_n = 1$  and is not of physical significance.

The importance of the length of the transition region for axial changes in the liner admittance was also examined. This provides a severe test of the wave-envelope method since finite axial changes occur over progressively shorter distances. From Table 3 one can see that the method properly calculates the transition to the discontinuous liner effects (the  $L=0$  case is obtained with the methods of Ref. 11). However, as  $L$  becomes smaller, a greater number of axial grid points are required to obtain accurate results; for  $L < 0.4$ ,  $(|d\beta/dx|_{\max} > .84)$  more than 50 axial steps of the Runge-Kutta procedure are required for the presented results, and the method becomes progressively less efficient with decreasing values of  $L$ . It is of interest to note that the magnitude of the transmission coefficients are nearly independent of the length of the transition region to the wavelength of the sound.

## V. Summary

A wave-envelope technique based on the method of variation of parameters has been developed; the basis of the analysis is an integrability constraint derived from the wave equation. The method represents the acoustic signal as a superposition of quasiparallel duct modes; this leads to direct calculation of the transmission and reflection coefficients of the variable-area segment and requires numerical calculation of only the slowly-varying mode amplitudes and phases. The advantage of the method in numerical efficiency has been demonstrated.

The results of a small perturbation theory are shown to be accurate for the direct transmission coefficients for wall slopes up to approximately 0.2; however, the theory does not adequately predict the intermodal coupling in transmission.

Reflection coefficients due to the variable area are found to be very small, with the exception of the direct reflection coefficient for a mode that is cut off in a converging section. The magnitude of the intermodal coupling in transmission due to axial variations of the liner properties is nearly independent of the rate of these variations.

## Appendix

The coefficients of Eqs. (13) and (16) involve several integrals across the duct width; letting

$$A_{mn} = \int_0^b y \sin \kappa_m y \cos \kappa_n y dy \quad (A1)$$

and

$$B_{mn} = \int_0^b y^2 \cos \kappa_m y \cos \kappa_n y dy \quad (A2)$$

and using the previous definition of  $N_n$ , Eq. (14), and  $E_n$ , Eq. (12), one can write the mode-coupling coefficients in the form

$$V_{mn} = (A_{mn} d\kappa_m/dx - A_{nm} d\kappa_n/dx) / N_n \quad (A3)$$

$$U_{mn} = [A_{mn} d^2 \kappa_m / dx^2 + (d\kappa_m/dx)^2 B_{mn} + (b \tan \theta d\kappa_m/dx + (1 - \cos \theta) \kappa_m / \cos \theta) \sin \kappa_m b \times \cos \kappa_n b] / N_n \quad (A4)$$

$$\tilde{V}_{mn} = (U_{mn} - V_{mn} i \kappa_m) / 2i \kappa_n E_m E_n \quad (A5)$$

and

$$\tilde{U}_{mn} = (U_{mn} + V_{mn} i \kappa_m) E_m / 2i \kappa_n E_n \quad (A6)$$

The integrals  $A_{mn}$  and  $B_{mn}$  are given by

$$A_{mn} = \frac{2\kappa_m N_m}{\cos \kappa_m b} \frac{\cos \kappa_n b}{\kappa_n^2 - \kappa_m^2}, \quad m \neq n \quad (A7)$$

$$B_{mn} = 2 \frac{\kappa_m A_{mn} - \kappa_n A_{nm}}{\kappa_n^2 - \kappa_m^2}, \quad m \neq n \quad (A8)$$

and

$$A_{nn} = (\sin 2\kappa_n b - 2\kappa_n b \cos 2\kappa_n b) / 8\kappa_n^2 \quad (A9)$$

$$B_{nn} = b^3 / 6 + (2\kappa_n^2 b^2 - 1) \sin 2\kappa_n b / 8\kappa_n^3 + b \cos 2\kappa_n b / 4\kappa_n^2 \quad (A10)$$

### Acknowledgment

This work was performed under support from NASA-Langley Research Center, Contract No. NAS 1-13884.

### References

- <sup>1</sup>Nayfeh, A. H., Kaiser, J. E., and Telionis, D. P., "Acoustics of Aircraft Engine-Duct Systems," *AIAA Journal*, Vol. 13, Feb. 1975, pp. 130-153.
- <sup>2</sup>Quinn, D. W., "A Finite Difference Method for Computing Sound Propagation in Non-Uniform Ducts," *AIAA Journal*, Vol. 13, Oct. 1975, pp. 1392-1394.
- <sup>3</sup>Nayfeh, A. H. and Telionis, D. P., "Acoustic Propagation in Ducts with Varying Cross-Section," *The Journal of the Acoustical Society of America*, Vol. 54, Dec. 1973, pp. 1654-1661.
- <sup>4</sup>Nayfeh, A. H., Telionis, D. P., and Lekoudis, S. G., "Acoustic Propagation in Ducts with Varying Cross Sections and Sheared Mean Flow," *Progress in Astronautics and Aeronautics: Aeroacoustics: Jet and Combustion Noise; Duct Acoustics*, Vol. 37, Editor: Henry T. Nagamatsu; Associate Editors: Jack V. O'Keefe and Ira R. Schwartz, MIT Press, Cambridge, Mass., 1975, pp. 333-351.
- <sup>5</sup>Nayfeh, A. H., Kaiser, J. E., and Telionis, D. P., "Transmission of Sound Through Annular Ducts of Varying Cross Sections and Sheared Mean Flow," *AIAA Journal*, Vol. 13, Jan. 1975, pp. 60-65.
- <sup>6</sup>Stevenson, A. F., "Exact and Approximate Equations for Wave Propagation in Acoustic Horns," *Journal of Applied Physics*, Vol. 22, Dec. 1951, pp. 1461-1463.
- <sup>7</sup>Eversman, W., Cook, E. L., and Beckemeyer, R. J., "A Method of Weighted Residuals for the Investigation of Sound Transmission in Non-Uniform Ducts without Flow," *Journal of Sound and Vibration*, Vol. 38, Jan. 1975, pp. 105-123.
- <sup>8</sup>Baumeister, K. J., "Generalized Wave Envelope Analysis of Sound Propagation in Ducts with Variable Axial Impedance and Stepped Noise Source Profiles," *Progress in Astronautics and Aeronautics: Aeroacoustics; Fan Noise and Control; Duct Acoustics; Rotor Noise*, Vol. 44, Editor: Ira R. Schwartz, Assistant Editors: Henry T. Nagamatsu and Warren C. Strahle, MIT Press, Cambridge, Mass., 1976, pp. 451-474.
- <sup>9</sup>Nayfeh, A. H., *Perturbation Methods*, Wiley-Interscience, New York, 1973, Chap. 5.
- <sup>10</sup>Finlayson, B. A., *The Method of Weighted Residuals and Variational Principles*, Academic Press, New York, 1972, pp. 7-12.
- <sup>11</sup>Zorumski, W., "Acoustic Theory of Axisymmetric Multisectioned Ducts," NASA TR R-419, 1974.